Chapter 4

Nanocomposites Based on Thermoplastic Polyester Elastomers

Sandra Paszkiewicz, Iman Taraghi, Anna Szymczyk, Elżbieta Piesowicz and Zbigniew Rosłaniec

Additional information is available at the end of the chapter

http://dx.doi.org/10.5772/intechopen.68216

Abstract

The use of fillers in order to enhance the properties of polymers has been already well documented. Fundamentally, traditional fillers were applied to reduce the cost of the final polymeric products. Moreover, most micron-sized fillers required high loading for slight properties enhancement, thus causing problems in processing and melt flow due to the high viscosity of the obtained composite. Nanofillers might constitute the answer to the requirements made to the modern polymer materials. Nanofillers in the range of 3–5 wt% achieve the same reinforcement as 20–30 wt% of micron-sized fillers. Therefore, this study presents the influence of three different types of nanofillers that differ in shape (aspect ratio) on the morphology, electrical conductivity, and thermal stability of polyester thermoplastic elastomer (TPE) matrix, by means of poly(trimethylene)-*block*-poly(tetramethylene oxide) copolymer (PTT-PTMO). The morphology in this copolymer consisted of semicrystalline PTT domains dispersed in the soft phase of amorphous, noncrystallisable PTMO. The PTT-PTMO copolymer has been combined with 0.5 wt% of 1D (single-walled carbon nanotubes (SWCNTs), silicon carbide (SiC) nanofibers), 2D (graphene oxide (GO), graphene nanoplatelets (GNPs)), and 3D (polyhedral oligomeric silsesquioxane (POSS)) through *in situ* synthesis to obtain nanocomposites (NCs) samples.

Keywords: polymer nanocomposites, thermoplastic elastomer, graphene derivatives, carbon nanotubes, SiC, POSS particles, *in situ* synthesis, electrical conductivity, morphology

1. Introduction

Thermoplastic elastomers (TPEs) belong to the widely studied group of polymers, which express characteristics of both thermoplastics and rubbery materials based on weight concentrations of each part [1–5]. Recently, the incorporation of nanofillers into the TPEs has been converted to a challenging issue for many researchers to obtain unique functional materials with superior mechanical, thermal, and electrical properties [6–16]. Organic and inorganic nanoadditives, such as three-dimensional (3D) fullerenes, polyhedral oligomeric silsesquioxanes (POSSs), carbon black (CB); two-dimensional (2D) graphene nanoplatelets (GNPs), montmorillonite (MMT); and one-dimensional (1D) carbon nanotubes and nanofibers (CNTs and CNFs), are widely used as fillers in order to obtain polymer composites with enhanced physical properties at a very low content of nanoparticles. However, the shapes and aspect ratios, amount of concentrations, and large scale of aggregation, dispersion, and orientation degree of the nanofillers are the main factors for the overall characteristics of the nanocomposites (NCs) [17–20]. Furthermore, the dispersion state of nanofillers in the NCs could be influenced by viscosity of the matrix [21]. Hence, providing the excellent dispersion state of nanofillers into the matrix is one of the factors that the scientists design and produce novel functional materials based on the TPEs.

Poly(ether-ester)s (PEEs), which are segmented blocks of copolymers consisting of alternating sequences of flexible polyether and rigid polyester segments, exhibit a TPE behavior. They are of special interest due to their excellent mechanical properties, such as strength and elasticity in a wide range of temperature. PEEs based on poly(butylene terephthalate) (PBT) as rigid segments, and poly(tetramethylene oxide) (PTMO) as soft segments (PBT-PTMO) are available as commercial products (Elitel™, Arnitel, Hytrel®, DSM, etc.). Recently developed polyester thermoplastic based on poly(trimethylene terephthalate) (PTT) as the rigid segment and PTMO as flexible ones (PTT-PTMO) were first synthesized and characterized by Szymczyk et al. [5]. PTT is a recently commercialized aromatic polyester, which has become one of the most important polymer materials, since DuPont obtained PTT (Sorona® EP), which contains 20–37% renewable material from nonfood biomass, and has performance similar to conventional PBT plastics [22]. Additionally, the incorporation of nanofillers with different shapes and aspect ratios into the PTT-PTMO matrix has been already studied [7, 10–16]. The main objective of those studies was to investigate the effect of the addition of various types of nanofillers on the mechanical, thermal, electrical, and viscoelastic properties of the PTT-PTMO. For instance, the incorporation of SWCNTs into the PTT-PTMO caused the significant increase in the values of the Young's modulus, yield stress, and elongation at break, while, the GNPs indicated the opposite effect on the mechanical properties of neat PTT-PTMO [11]. Moreover, the presence of SWCNTs and GNPs in the polymer speeded up the crystallization process as it was evidenced by a shift of the crystallization peak to up to 45°C, which was recorded for the hybrid nanocomposite that contained 0.5 wt% of SWCNTs and 0.1 wt% of GNPs. Furthermore, the addition of SWCNTs and GNPs individually, as well as the mixture of both, caused substantial enhancement of thermooxidative stability, shifting the beginning of the chemical decomposition temperature by 20–25°C [11]. At the same time, a remarkable synergistic effect between GNPs and SWCNTs leading to an improvement of the electrical and thermal conductivities of the PTT-PTMO/GNPs/SWCNTs hybrid NCs was observed [10, 12]. Despite the fact that PTT-PTMO/GNPs nanocomposites were

found to be nonconductive at a total content of 0.1 and 0.3 wt%, which was perhaps due to large number of defects, free radicals, and other irregularities on the surface of nanoplatelets [12], a significant synergistic effect between SWCNTs and GNPs on improving electrical conductivity of nanocomposites based on segmented block copolymers has been observed. Moreover, ceramic silicon carbide (SiC) nanofibers, which improve electron mobility and thermal conductivity, and at the same time, ensure chemical and high temperature resistivity [23–25], can be a good candidate as a 1D nanostructure to combine with novel polymeric materials to be used in photovoltaic utilizations. For instance, Mdletsche et al. [16] has investigated the efficiency of the addition of SiC nanoparticles on the mechanical, thermal, and biodegradation properties of polycaprolactone. Moreover, the effect of GO as 2D nanofillers on the phase structure, melt viscosity, and the mechanical properties of PTT-PTMO was studied by the means of DSC, ARES rheometer, and tensile tests [11]. An improvement of the Young's modulus and yield stress was observed in the PTT-PTMO/GO NCs with the increase of GO content from 0 to 0.5 wt% [11]. Such an improvement was observed most probably due to the large interfacial area and high aspect ratio of GO. Furthermore, the effects of POSS particles on the phase separation and glass transition temperature (T_g) of the PTT-PTMO has been investigated using dynamic mechanical thermal analysis (DMTA) [15]. POSS affected the phase separation of the polymer matrix, and it was shown that the glass transition temperature of PTMO-rich soft phase, melting temperature of PTT hard phase, and the degree of crystallinity of the nanocomposites were not affected by the presence of POSS cages in PTT-PTMO matrix. The crystallization temperatures shifted from 154°C for the neat copolymer to 130–133°C for nanocomposites. This was indicated on the anti-nucleating behavior of POSS particles for crystallization of PTT hard phase [15].

The main objective of this chapter is to compare the influence of nanofillers that differ in shape (aspect ratio) on the supramolecular structure, phase separation, thermal stability, and electrical conductivity of the PTT-PTMO-based nanocomposites. The 1D (SWCNT, SiC), 2D (GO, GNP), and 3D (POSS) type nanofillers were selected to be mixed with the polymer matrix. The next sections exhibit complete discussion of the present study.

2. Materials and methods

2.1. Materials and synthesis

For the manufacturing process of the PTT-PTMO copolymers, the dimethyl terephtalate (DMT, Sigma Aldrich), 1,3-propanenediol (PDO, Sigma Aldrich), and poly(tetramethylene oxide) glycol (PTMG) with the molecular mass of 1000 g/mol (DuPont, United States) were used. Tetrabutyl orthotitaniate (TBT, Fluka) was applied as a catalyst in transesterification and polycondensation steps. Irganox 1098 (Ciba-Geigy, Switzerland) was used as an antioxidant.

Moreover, the selected nanofillers, which were described in details in Refs. [10–15, 26] have been listed as follows: SWCNTs with a diameter of <2 nm, length of 5–30 μm, purity higher than 95%, and surface area of 380 m^2/g were bought from Grafen Chemical Industries, Grafen Co., Ankara, Turkey [10–12]; SiC nanofibers were produced via self-propagating high-temperature synthesis (SHS) from elemental Si and poly(tetrafluoroethylene) (PTFE) powder mixtures and provided

by the group of Prof. A. Huczko [26]; GNPs in the form of a powder with less than three graphene layers, x–y dimensions of up to 10 μm, carbon content of ~97.0%, and the oxygen content of ~2.10% were bought from ANGSTRON Materials, Dayton, Ohio, USA [10–12]; GO sheets with average particle size of 50 μm obtained from expanded graphite (SLG Technologies GMbH, Germany) by Brodie oxidation method [27] were provided by the Polymer Institute of Slovak Academy of Science) [10, 11]; octakis[(n-octyl)dimethylsiloxy]octasilsesquioxane (POSS) was obtained according to a sequential methodology presented in scheme in Ref. [12] and provided by the Centre for Advanced Technologies, Poznan, Poland). The neat PTT-PTMO copolymer and PTT-PTMO-based NCs were produced by *in situ* polymerization technique. The procedure details were already published elsewhere [7–12]; however, the scheme of the synthesis process is presented in **Figure 1**. First, the nanofillers were dispersed for 30 min using high-speed stirrer device (Ultra-Turax T25) and ultrasonicator apparatus (Homogenizer HD 2200, Sonoplus, with frequency of 20 kHz and power 200 W) in PDO. Then, the polymerization process conducted in two stages has been applied. In the first stage, the dispersion of the selected nanofiller in PDO, DMT, and TBT catalyst were charged into 1 dm^3 steel reactor (Autoclave Engineers Inc, USA), where DMT was transesterified with PDO in the presence of catalyst under nitrogen flow at 165°C and atmospheric pressure under nitrogen flow. PDO was used in a sixfold molar excess over DMT. During the reaction, methanol was distilled off. After ca. 1.5 h to the reaction mixture, comprises mostly of *bis*-(3-hydroxypropyl) terephthalate, the PTMG, Irganox 1010, and second portion of catalyst were added. Then, the temperature was slowly lifted up to 210°C and

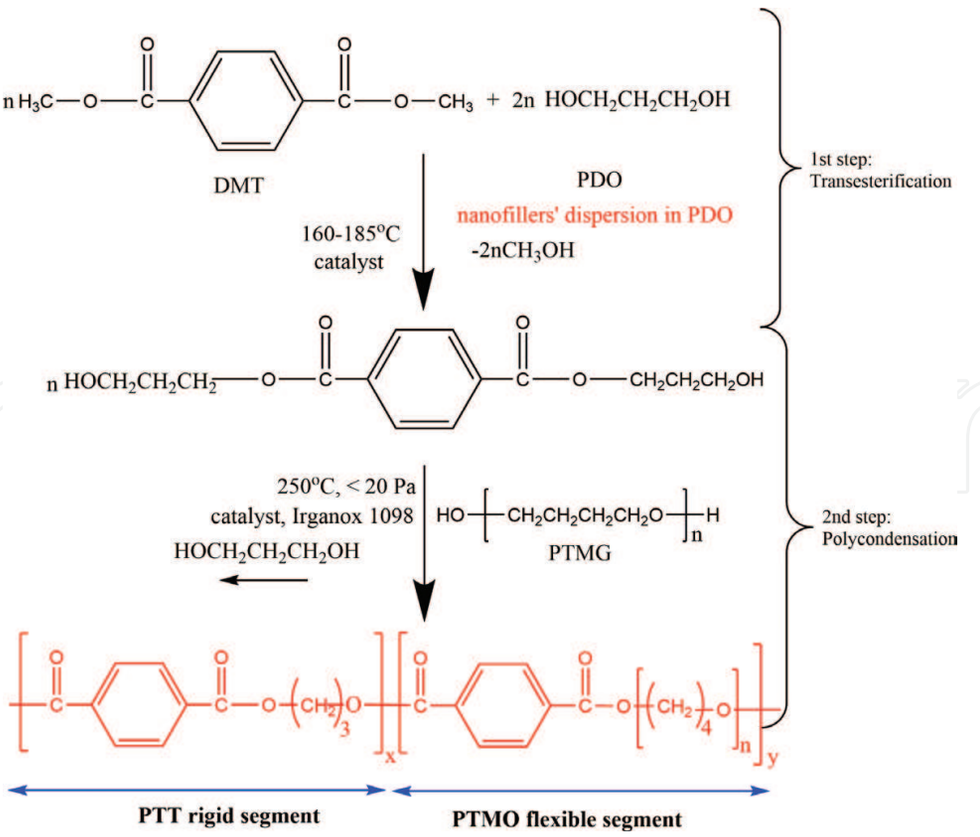

Figure 1. Scheme of the preparation process of PTT-PTMO and PTT-PTMO-based nanocomposites.

held to reach the endpoint of transesterification. Subsequently, the excess of PDO, used in the first stage, was distilled off during increasing the temperature and reducing the pressure. The second step, melt polycondensation was carried out at 250°C under reduced pressure of ~20 Pa. During polycondensation, the torque was monitored in order to detect changes in viscosity. All syntheses were finished when the melt reached the same value of viscosity at 250°C. The obtained PTT-PTMO and PTT-PTMO NCs were extruded from the reactor under nitrogen flow. The content of rigid PTT and flexible PTMO segments was approximately the same (i.e., 50 wt% of each). Finally, the extruded neat PTT-PTMO and NCs were granulated, injection molded, and compressed to prepare the specimens in accordance to the standard tests.

2.2. Characterization methods

The SEM analyses have been applied using two different scanning electron microscopes (SEM, JEOL JSM 6100; SEM ULTRA-55 Zeiss and SEM SUPRA-55 VP Zeiss). Before SEM evaluation, the extruded specimens were cryo-fractured in liquid nitrogen and then fractured surfaces were coated with thin gold layers.

In order to evaluate DMTA analysis, a Polymer Laboratories MK II apparatus has been applied in the bending mode at the constant frequency of 1 Hz and a heating rate of 3°C/min from −100°C to the sample softening temperature.

The thermal behavior was observed using differential scanning calorimetry (DSC, TA Instrument Q-100) at the heating and cooling rates of 10°C/min in the heating-cooling-heating cycle. Cooling and second heating were used in order to determine melting and crystallization temperatures. The heat of fusion was determined by integration of the normalized area of melting endotherm. The procedure of calculation degree of crystallinity and determination of glass transition temperature was already published in Refs. [5, 7, 10–12].

The electrical conductivity measurements were conducted by a Novocontrol broadband dielectric spectrometer. The complex permittivity $\varepsilon^* = \varepsilon' - i\varepsilon''$, where ε' indicates the permittivity and ε'' the dielectric loss, which was operated as a function of frequency ranging from 10^{-2} Hz < F < 10^6 Hz. The broadband electrical conductivity is usually represented as $\sigma(F) = \sigma_{DC} + \sigma_{AC} = \sigma_{DC} + A\cdot(F)^S$, where σ_{DC} is the frequency independent direct current (DC) conductivity, caused by the movement of electrons in phase with applied electric field. $A\cdot(F)^S = \sigma_{AC}$ is the component of conductivity associated with alternating current (AC), where F is frequency. The electrical conductivity of the samples was derived by $\sigma(F) = \varepsilon_0 2\pi F \varepsilon''$, where ε_0 is the vacuum permittivity [12]. Among all of the NCs specimens, the PTT-PTMO/POSS NC was not considered for the dielectric measurements, since the electrical conductivity of PTT-PTMO matrix as a host polymer cannot be influenced by the POSS nanoparticles.

Thermal and thermooxidative stability of the prepared polymer nanocomposites were evaluated by thermogravimetry (TGA 92-16.18 Setaram) at simultaneous TG-DSC system. Measurements were carried out in inert atmosphere (argon) and an oxidizing atmosphere, that is, dry, synthetic air (N_2:O_2 = 80:20 vol.%). The study was conducted at the heating rate of 10°C/min in the temperature range of 20–700°C. Measurements were conducted in accordance with the PN-EN ISO 11358:2004 standard.

3. Results and discussion

3.1. Nanocomposite morphologies

In this part, the morphologies of the produced nanocomposites were investigated by means of scanning electron microscopy (SEM). SEM is a useful tool to give a distinct insight into the nanocomposite morphology and for assessing the dispersion of nanoparticles. Especially for conductive nanoparticles, such as SWCNTs, SiC, GNPs, and contrast imaging techniques, one can use this to visualize the nanoparticles networks due to a different state of charge of the matrix and nanoparticles [28–30].

Figure 2a–e has indicated the SEM images of PTT-PTMO-based nanocomposites with 0.5 wt% of SWCNTs, SiC, GO, GNPs, and POSS nanofillers, respectively. SEM analysis presents the well-dispersed nanoparticles in the whole volume of polymer matrix, and thus the micrographs confirm that *in situ* polymerization is a highly efficient method for preparing NCs. In **Figure 2a**, it is obvious that the SWCNTs were uniformly distributed in the PTT-PTMO matrix. Moreover, the fractured surface of PTT-PTMO/0.5SWCNT indicates that the SWCNTs were pulled-out from the matrix and still embedded at both ends in the matrix. It reveals the high potential of the SWCNTs to enhance the mechanical properties of the polymer nanocomposite [11]. Similarly, in the case of the SiC nanofibers, well-distributed nanoparticles with no obvious agglomerations were observed (**Figure 2b**). Moreover, most of the SiC NFs were embedded in the polymer matrix with both ends, just like the previously reported SWCNTs. Thus, the SEM

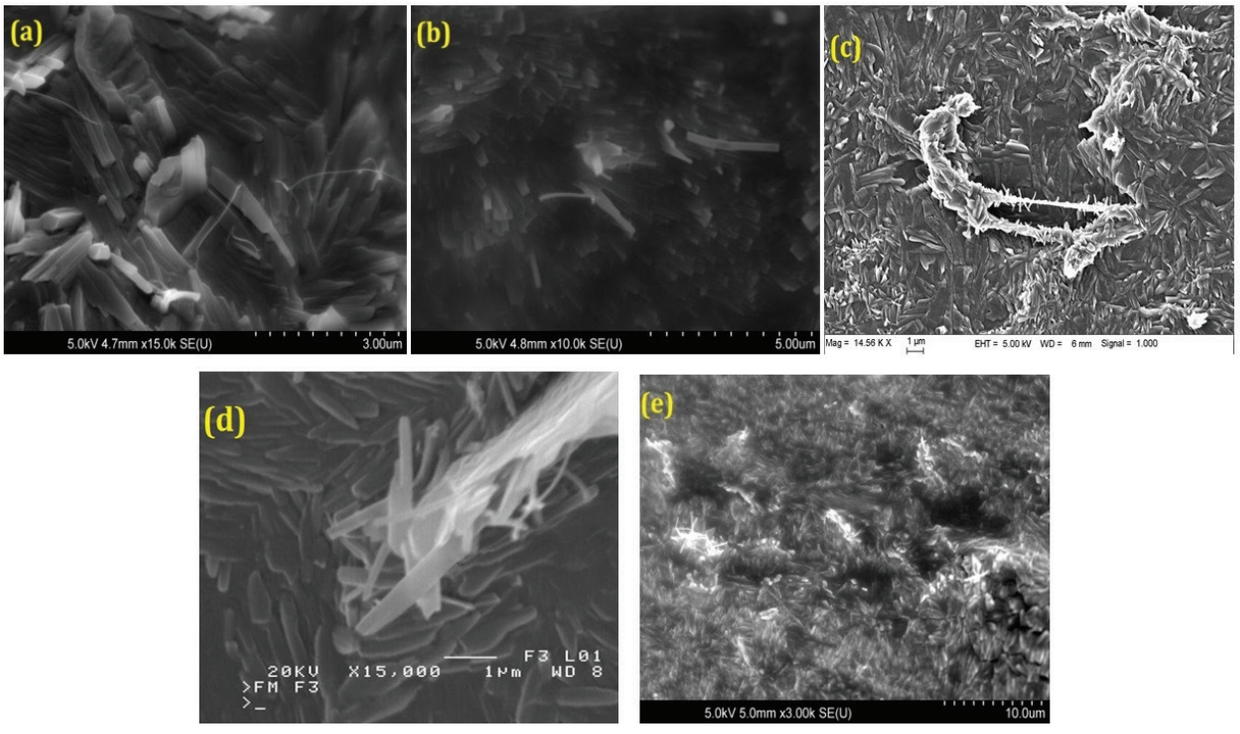

Figure 2. The SEM micrographs of PTT-PTMO copolymer reinforced with 0.5 wt% of (a) SWCNTs, (b) SiC, (c) GO, (d) GNP, and (e) POSS nanofillers.

images of NCs surface suggest the "pulling out" SiC NFs from the polymer matrix during the brittle fracture of the sample [10]. Thus, it can be concluded that 1D type nanofillers, that is, SWCNTs, SiC NFs, with high aspect ratio distinctly represent their efficiency for avoiding the existence of agglomerates due to the high shear mixing with high-frequency vibration [10–12, 26], thus confirming the legitimacy of the use of *in situ* method to obtain nanocomposites.

In the case of PTT-PTMO nanocomposites containing 2D-type nanofillers, that is, GNP and GO (**Figure 2c** and **d**, respectively), equally good dispersion was obtained. The PTT-PTMO/0.5GNPs nanocomposite (**Figure 2c**) indicates the presence of lower interfacial interactions between the GNPs and polymer matrix that is due to the existence of defects, free radicals, and other regularities on the surface of graphene nanosheets [12]. Additionally, the observations on the dispersion of GNPs were expanded upon Raman spectroscopy [12] and transmission electron microscopy (TEM) [13]. Since in our case, the Raman spectrum [12] of GNPs resembled the spectrum of reduced graphene oxide [31, 32], one could have expected strong interfacial interactions between GNPs and polymer matrix. Furthermore, in the case of PTT-PTMO/0.5GNPs [13] nanocomposite, the bent or crumpled/wrinkled platelets were visible. Exfoliated graphene-based materials are often compliant, and when dispersed in a polymer matrix are typically not observed as rigid disks (flat platelets), but rather as wrinkled ones. Moreover, randomly oriented, exfoliated platelets were observed, possibly due to restacking of the platelets. Ipso facto, the good dispersion of GO was also visible in **Figure 2d**, that it can result from the excellent dispersion of GO in PDO at the level of individual sheets. During *in situ* polymerization, a stable interphase interaction between GO nanofillers and PTT-PTMO copolymer was created due to the strong connections among the oxygen-containing functional groups [33–35] through the polymer [14]. Therefore, extreme reinforcement effects [14] were observed, while GO nanofillers were added in the polymer matrix without exhibition of agglomerates.

Finally, from the SEM image of PTT-PTMO/0.5POSS (**Figure 2e**), one can clearly see that the (n-octyl)dimethylsiloxy groups of POSS can react with functional groups of the matrix during *in situ* polymerization process. Therefore, POSS nanofillers can be completely connected to the PTT-PTMO due to excellent interfacial adhesion [15]. Such a study expanded upon SEM-EDX analysis [15] and provided the detailed insight into the distribution of POSS cages in the PTT-PTMO matrix along with the confirmation on the homogeneity in the silica distribution in the whole volume of polymer matrix.

Moreover, in our previous works [11, 13], the relation between dispersion of the nanofillers within the matrix and the values of melt viscosity has been verified and well discussed through the morphological studies. One can find that various shapes and aspect ratios could affect the values of melt viscosity, and consequently, the dispersion quality and orientation of the nanofillers in the polymer matrix.

3.2. Phase structure of PTT-PTMO-based nanocomposites

The phase structure of PTT-PTMO-based nanocomposites resulting from the addition of different types of nanofillers at the same content of 0.5 wt% was investigated by dynamic mechanical thermal analysis (DMTA). Temperatures of β_2-relaxation ($T_{\beta 2}$) and β_1-relaxation

($T_{\beta 1}$) were designated from the maximum of the loss modulus change curve and the loss angle tangent of temperature curve. Herein, the storage modulus (*E′*), loss modulus (*E″*), and tan *δ* for PTT-PTMO and PTT-PTMO-based nanocomposites are shown in **Figure 3a–c**, respectively. At a low temperature, an obvious inflection on the *E′* curves (related with the β_1 in the *E″* plot) can be observed, that is associated with the glass transition of the soft polyether-rich phase. At the temperature range between 20 and 120°C, a decrease and a subsequent increase in the quantities of *E′* was perceived which is due to the changes associated with the glass transition temperature of amorphous polyester (PTT) phase which is followed by cold crystallization. Moreover, the addition of carbon nanofillers into the multiphase block copolymer initiated the heterophase structure with one crystalline and two amorphous phases [11]. The elastic features of the segmented block copolymer result from the aforementioned microseparated phase structure, which is a result of the chemical nature and incompatibility between the rigid and flexible blocks/segments build into the polymer chains.

As a result, at a lower temperature, the increase in the values of *E′* was only observed for the PTT-PTMO/0.5GO; however, the *E′* decreased with the addition of SWCNT, SiC, GNP, and POSS. Above 20°C, the storage modulus depends on the type and amount of nanofillers, in

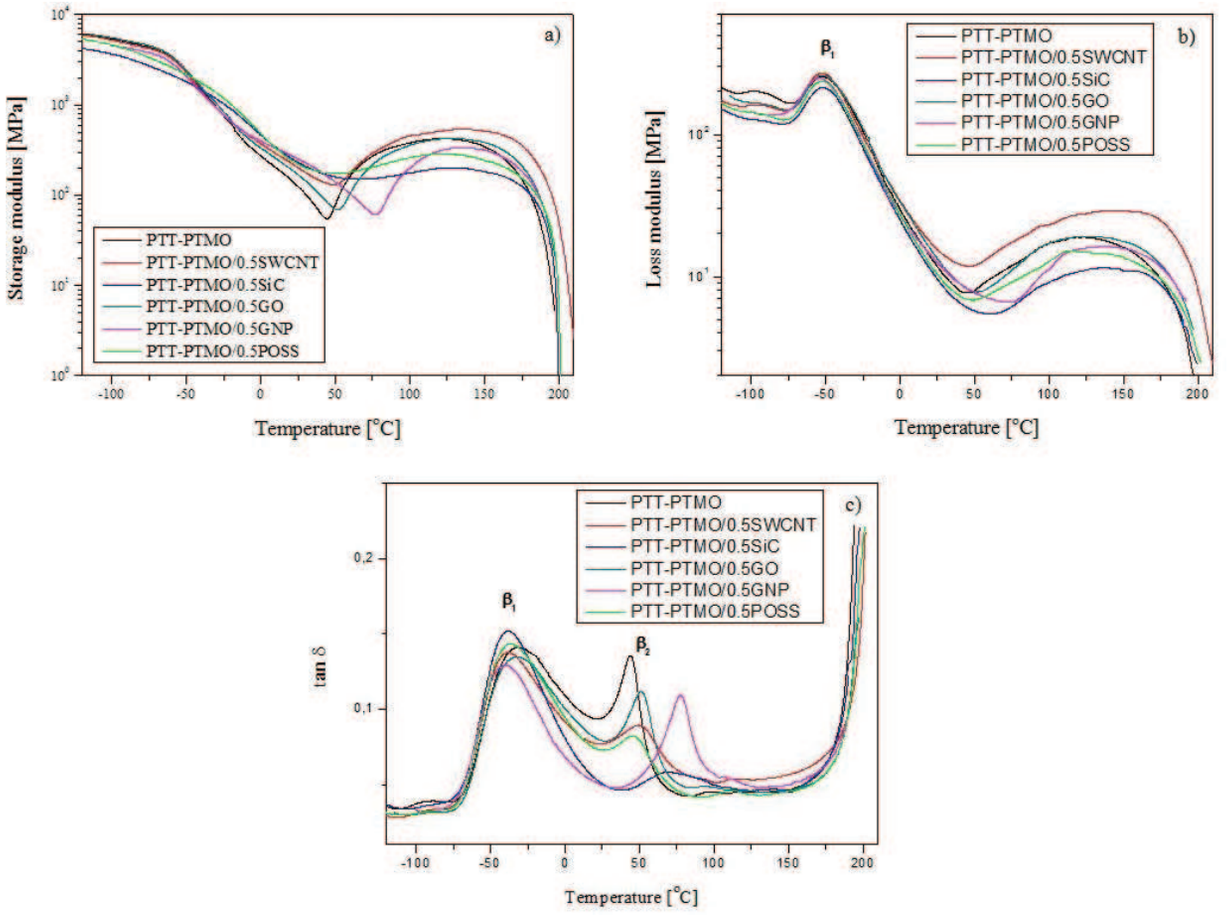

Figure 3. Rheological behavior of the PTT-PTMO copolymer and its nanocomposites (a) *E′*, (b) *E″*, and (c) tan *δ* as a function of temperature at frequency 1 Hz.

which the highest quantities of solid-like behavior for the nanocomposites were obtained with introduction of SWCNTs into the PTT-PTMO, which was probably due to the higher stiffening effect of the rigid SWCNTs and their extremely high modulus [36–39]. At peak β_1, the difference in the values of the peaks height is due to the variety effects of nanofillers on the mobility of the chains in the polymer matrix. SWCNTs caused the greatest molecular motions in comparison to the other nanofillers. This may come from the strong connection of SWCNTs with PTT-PTMO matrix (confirmed previously by TEM and Raman spectroscopy [10, 12]). In **Figure 3c** (tan δ curves), the β_1 and β_2 relaxation peaks are related to the glass transition of amorphous polyether phase and amorphous polyester phase, respectively [11]. The incorporation of carbon nanofillers into this polymer caused stronger phase separation as evidenced by a shift in the β_1 relaxation peak toward lower temperatures. In this case, at higher temperature, the GO nanoparticles exhibited the highest impact for the efficiency on the phase separation of the PTT-PTMO copolymer, comparing with other nanofillers such as SWCNT, SiC, GNPs, and POSS. And since, for PTT-PTMO/GO nanocomposites, an increase of long period (L) was observed [14], which resulted from an increase of amorphous layer thickness that was caused by the restriction of mobility of polymer chain, one can confirm that the addition of GO-induced interfacial interactions between polymer and nanosheets in the stronger manner. Moreover, in all of nanocomposites, the composition of each phase has taken place in the matrix, since the β_2 peak showed the smaller and wider peaks.

Additionally, the DSC analyses performed for the series of PTT-PTMO-based nanocomposites (**Table 1**) confirmed that the glass transition temperature of amorphous part in semicrystalline PTT hard phase (T_{g2}) of nanocomposites remained unaffected by incorporation of SWCNT, GNP, GO, and POSS nanoparticles. At the same time, regardless of the effect of the addition of nanoparticles on the melting temperature (T_m), a slight increase (2–6°C) was observed, while the degrees of crystallinity of the prepared nanocomposites were comparable to the neat PTT-PTMO block copolymer. At the loading of 0.5 wt% SiC, GO, GNP, and POSS in PTT-PTMO matrix, the values of crystallization temperatures (T_c) of nanocomposites were close to the T_c of neat PTT-PTMO [11, 14, 15]. The only exception was the nanocomposite that contains 0.5 wt% of SWCNTs that accelerated the rate of crystallization probably due to affinity of nanotubes to act as crystallization agents. These states in agreement with many studies [40–45] proved that SWCNTs are the strongest nucleation agents.

3.3. Electrical conductivity of nanocomposites

Polymer nanocomposites based on carbon nanoparticles have enjoyed a big interest due to their enhanced mechanical and thermal properties along with electrical and thermal conductivity. In particular, nanocomposites based on carbon nanotubes (CNT), both SWCNTs and MWCNTs, carbon nanofibers, like SiC NFs [24, 26, 46], as well as graphene derivatives like GNP or expanded graphite (EG) have shown to exhibit exceptional mechanical strength and electrical conductivity [47–55]. In turn, in order to restore the electrical conductivity of

Sample	T_{g1}	T_{g2}	T_m	ΔH_m	T_c	ΔH_c	x_c	Reference
	°C	°C	°C	J/g	°C	J/g	%	
PTT-PTMO	−58	53	206	30.9	126	28.3	21.2	[69]
PTT-PTMO/0.5SWCNT	−63	54	206	34.6	171	34.5	24.9	[69]
PTT-PTMO/0.5SiC	−64	–	206	30.1	153	29.7	21.7	–
PTT-PTMO/0.5GO	−67	54	204	31.5	123	32.0	22.7	[14]
PTT-PTMO/0.5GNP	−67	53	203	34.3	148	34.2	24,7	[69]
PTT-PTMO/0.5POSS	−68	54	207	34.2	131	30.3	24.6	[15]

T_{g1}: glass transition temperature of soft phase; Tg_2: glass transition temperature of hard phase; T_m: melting temperature of polyester crystalline phase; T_c: crystallization temperature of polyester crystalline phase; ΔH_m, ΔH_c: enthalpy of melting and crystallization of polyester crystals, respectively; x_c: mass fraction of crystallinity.

Table 1. Thermal properties of neat PTT-PTMO and PTT-PTMO-based nanocomposites determined by DSC.

http://dx.doi.org/10.5772/intechopen.68216

GO nanosheets, at least partial reduction is needed [18], since it is electrically insulating and thermally unstable. Therefore, in this work, the electrical conductivity of PTT-PTMO/0.5GO nanocomposite was also investigated, since during the synthesis process some partial reduction (second step of the synthesis takes place at 250°C) could have appeared. The use of *in situ* polycondensation method allows to obtain conductive nanocomposites filled with a relatively low loading (less than 0.5 wt%), which has been confirmed for the many types of polymer matrices [56–59]. **Figure 4** shows the alternating current electrical conductivity (σ) as a function of frequency (F) for PTT-PTMO nanocomposites and neat PTT-PTMO copolymer (reference sample).

PTT-PTMO block copolymers show at low frequencies characteristic conducting behavior (the presence of a frequency independent component, σ_{dc}) associated with the presence of PTMO. Such behavior may be due to ionic conductivity [60]. According to the results, the creation of the conducting paths in the insulating PTT-PTMO copolymer was strongly influenced by the presence of carbon nanofillers. The electrical conductivity of the nanofillers plays a main role to produce conductive polymer nanocomposites. POSS nanoparticles can improve the dielectric properties of the materials; however, this improvement is attributed to various factors, such as large particle-polymer interfacial area, particle-polymer nanoscopic structure, change in internal electric field (polarity) due to the presence of nanoparticles, functionality [61–63]), herein only the effect of carbon nanofillers on the electrical conductivity of the PTT-PTMO copolymer was investigated. In order to obtain higher electrical conductivity at lower cost, several factors need to be

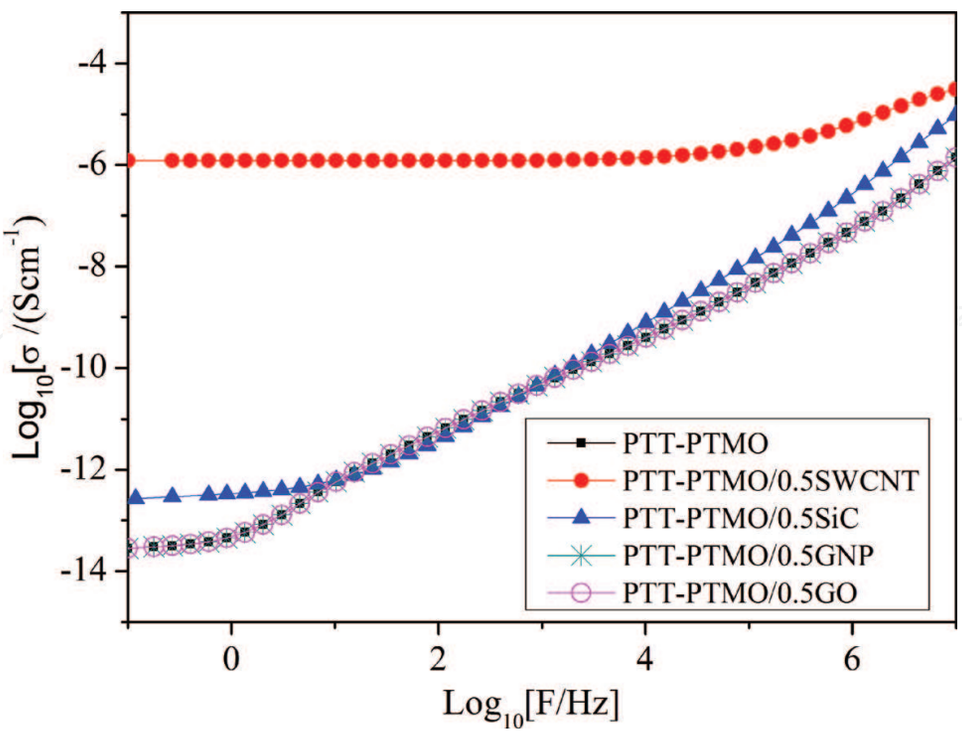

Figure 4. Broadband electrical conductivity ($\sigma(F)$) as a function of frequency (F) at room temperature for neat PTT-PTMO and its nanocomposites.

taken into consideration, that is, proper dispersion, orientation degree, and the amounts of agglomerates within the polymer-based nanocomposites [64–66]. The study of the broadband electrical conductivity confirms that the incorporation of the SWCNTs into the PTT-PTMO can covert the insolating polymers with two rigid and soft phases to the conductive specimens. The incorporation of 0.5 wt% of SWCNTs was high enough to provide conductive paths in the polymer matrix. However, even with the smaller loading of nanoparticles (0.1 wt% of SWCNTs), a slight increase in conductivity was observed, similarly as in the case of 0.3 wt% of SWCNTs [12]. Unlike SWCNTs, the GNPs and GO could not affect the electrical conductivity of the PTT-PTMO copolymer in the same manner. Due to the existence of rich defects, free radicals, residual functional groups, and impurities on the surface of GNPs, the percolation threshold has not taken place in PTT-PTMO/GNPs nanocomposites [10, 12]. However, by the way, it is also worth mentioning that conducting networks in PTT-PTMO block copolymer was already formed at 0.3 wt% of SWCNT alone [12], and further increase of 0.1 wt% of GNPs provided more electron pathways by synergy between the SWCNTs and GNPs. Once the filler content exceeded the percolation threshold, agglomerates could have even improved the electrical conductivity than well-dispersed CNTs. Along with an increase of the SWCNTs to GNPs content ratio to 5:1 (PTT-PTMO/0.5SWCNTs + 0.1GNPs), one observed the characteristic flat plot, where an extended frequency region of constant σ was detected [12]. The hybrid PTT-PTMO/0.5SWCNTs + 0.1GNPs exhibited the typical behavior for semiconducting samples with conductivity of about 10^{-6} S/cm. These observations made for the improvement in electrical conductivity of PTT-PTMO/SWCNT by GNPs were supported by the fact that the GNPs' surface rich of defects, free radicals, and other irregularities ensured strong nanotube-to-nanoplatelet interactions. These results highlighted the remarkable potential in industrial application of a new group of polymer hybrid nanocomposites, based on nanofillers with different shapes (SWCNTs and GNPs).

In addition, as mentioned above, GO nanosheets cannot create electric paths through the polymer due to the presence of functional groups such as –COOH and –OH on its surface [33–35]. Even the high temperature during *in situ* synthesis did not restore the conductivity of GO, thus the nanocomposite with 0.5 wt% of GO was found to be not conductive. Moreover, as shown in **Figure 4**, for nanocomposites with SiC nanofibers, the values of electrical conductivity in low frequency range exhibit higher values than those of pristine matrix. This fact suggests that there are many connections between nanofibers, with small gaps of polymer between them, which promotes polarization phenomena [26]. Our further study on the electrical properties of PTT-PTMO/SiC nanocomposites with higher content of SiC confirmed the electrical percolation threshold (ϕ_c) equals to 1.7 [26]. Additionally, the calculated critical exponent "*t*" [67] (equaled to 1.7) proved that a three-dimensional system was obtained [68]. Despite the fact that this study deals with nanocomposites based on PTT-PTMO block copolymer, with the total concentration of 0.5 wt%, it should be mentioned that the rather low percolation threshold, the low cost of preparation of SiC nanofibers compared to nanocomposites containing SWCNTs (ca. 1000 USD/kg for SiC nanofibers and about hundreds USD/g

for SWCNT) [69–71], and their low viscosity values, which makes it easier for extrusion process after *in situ* method, give rise to a new class of interesting materials with potential use in a wide range of applications.

3.4. Thermal stability of nanocomposites

The incorporation of nanofillers with high thermal conductivity into polymer matrix may facilitate heat distribution in the material and thereby improve its heat resistance. Most carbon nanostructures, such as CNTs, SiC, and graphene derivatives, exhibit electron affinities similar to those of fullerenes, and they are therefore capable of acting as radical scavengers in free radical chain reactions, including polymerization and the thermo-oxidative degradation of polymers [69, 72]. Similarly, several studies confirmed that the incorporation of POSS can enhance the thermal stability of nanocomposites [61, 62]. The influence of the presence of SWCNT, SiC, GNP, GO, and POSS particles on the thermal and thermo-oxidative decomposition of the nanocomposites based on PTT-PTMO block copolymer has been investigated during heating in air and argon atmosphere. The weight loss (TG) and its derivative of weight loss (DTG) curves are shown in **Figure 5a** and **b**. The mechanisms of thermal and thermo-oxidative degradation of copoly(ether-ester) have been already widely discussed [73, 74]. Decomposition of copoly(ether-ester) begins with the flexible segment PTMO. Oxygen mainly affects the carbon atom located in the α position relative to the ether oxygen atom in ether [73]. Detailed studies have been done for PBT-PTMO copolymers, however, for the PTT-PTMO, the mechanism is identical, differing only in decay fragments. The thermal decomposition process of poly(1,4-tetraoksymethylene) (PTMO) chains has a radical nature, and in the initial stage of PTMO chain decomposition is observed the secretion of tetrahydrofurane (THF) aldehydes and low-boiling and volatile alkenes. At the temperature of 200°C occurs the thermal oxidation of PTMO segment with releasing volatile substances [69]. An analysis of the values of the characteristic temperatures of decomposition, including the temperature of 5, 10, and and 50% weight loss and the temperature at the maximum weight loss rate (T_{DTG}) of neat PTT-PTMO and PTT-PTMO nanocomposites (**Table 2**) showed that the presence of different types of nanofillers at the concentration of 0.5 wt% does not affect the thermal stability in an inert atmosphere (**Figure 5b**), regardless of nanofillers' content, whereas in oxidizing atmosphere, an effect on thermo-oxidative stability of the polymer matrix has been observed. The studies on thermal decomposition of PTT-PTMO nanocomposites proved that in an oxidized atmosphere, the thermal degradation process proceeds in two steps (**Figure 5a**), whereas in inert atmosphere, proceeds in only one step (**Figure 5b**). Thermal degradation profiles of PTT-PTMO nanocomposites displayed that thermal stability of the nanocomposites based on SWCNT and graphene derivatives (GO and GNP) was improved at the concentration of 0.5 wt%, while the incorporation of 0.5 wt% of SiC NFs and POSS particles caused a decrease in thermal stability of PTT-PTMO nanocomposites at the first stage of decomposition process (values of $T_{5\%}$ and $T_{10\%}$). In turn, the values of $T_{50\%}$ for the whole series of PTT-PTMO-based nanocomposites were comparable to one another.

Only in the case of PTT-PTMO/SWCNT composite, do the thermal degradation temperatures increase to about several degrees. Furthermore, the values of the temperature at the maximum weight loss rate (T_{DTG2}) of neat PTT-PTMO and PTT-PTMO nanocomposites containing SWCNT and graphene derivatives suggested the strongest effect on the thermal stabilization behavior. Since all nanofillers are found to be well-dispersed in PTT-PTMO matrix (**Figure 2**), carbon nanotubes and graphene derivatives caused the annihilation of free radicals gener-

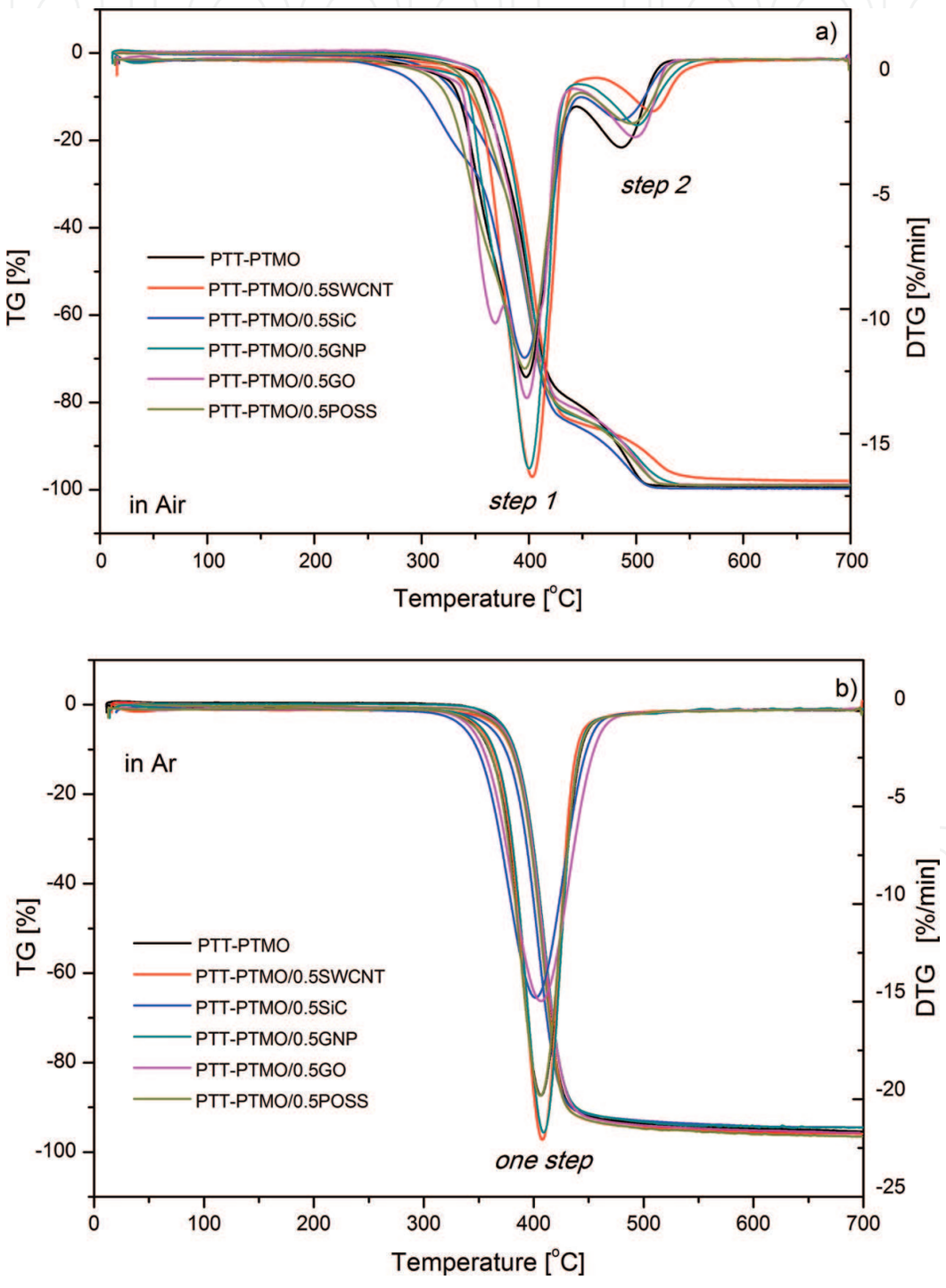

Figure 5. Weight loss and derivative weight loss versus temperature for neat PTT-PTMO and PTT-PTMO-based nanocomposites in air (a) and in argon (b) at a heating rate of 10°C/min.

ated during thermal decomposition of polymer matrix in nanocomposite in the strongest manner, and thus retarding thermal degradation of the nanocomposites.

Symbol	$T_{5\%}$, °C	$T_{10\%}$, °C	$T_{50\%}$, °C	T_{DTG1}, °C	T_{DTG2}, °C
Measurement carried out in an oxidizing atmosphere					
PTT-PTMO	347	358	398	397	485
PTT-PTMO/0.5SWCNT	350	369	402	403	516
PTT-PTMO/0.5SiC	315	333	394	395	486
PTT-PTMO/0.5GNP	356	365	399	400	502
PTT-PTMO/0.5GO	353	360	396	368/397	501
PTT-PTMO/0.5POSS	336	350	395	395	496
Measurement carried out in argon					
PTT-PTMO	371	382	407	406	–
PTT-PTMO/0.5SWCNT	367	380	406	408	–
PTT-PTMO/0.5SiC	360	374	403	401	–
PTT-PTMO/0.5GNP	373	383	409	410	–
PTT-PTMO/0.5GO	371	381	408	406	–
PTT-PTMO/0.5POSS	369	380	406	406	–

Table 2. Temperatures corresponding to 5, 10, and 50% weight loss and the temperature at maximum of weight loss rate for PTT-PTMO and PTT-PTMO-based nanocomposites obtained in an air and argon atmosphere.

4. Conclusions

PTT-PTMO block copolymer-based nanocomposites were prepared by *in situ* polymerization with an addition of 0.5 wt% of several types of nanofillers, that is, SWCNTs, SiC, GO, GNP, and POSS nanoparticles. SEM micrographs verified that the dispersion of the nanofillers in the PTT-PTMO matrix was rather homogeneous suggesting that *in situ* polymerization is a highly efficient method for preparing nanocomposites with low loading of nanofillers. DMTA has been used in order to investigate the effect of nanofillers on the phase separation and phase transition temperatures ($T_{\beta1}$, $T_{\beta2}$) of the thermoplastic elastomer matrix. One can conclude that both, organic and inorganic nanofillers affected the phase separation of PTT-PTMO block copolymer. Additionally, it was observed that PTT-PTMO/0.5GO and PTT-PTMO/0.5GNP were found to be nonconductive. In turn, a conducting network has been formed by 0.3 wt% of SWCNT. While in the case of PTT-PTMO nanocomposites containing SiC, the percolation threshold equals to 1.7 wt%. Moreover, SWCNT and graphene derivatives caused the annihilation of free radicals generated during thermal decomposition in oxidizing atmosphere of polymer matrix in nanocomposites in the strongest manner, and thus retarding thermal degradation of the nanocomposites, in comparison to the effect of SiC NFs and POSS particles, while in an inert atmosphere no significant influence due to the addition of nanofillers that differ in shape was observed.

Acknowledgements

This work is the result of the research project GEKON2/O5/266860/24/2016 funded by The National Centre for Research and Development and National Fund for Environmental Protection and Water Management, Poland.

Author details

Sandra Paszkiewicz[1]*, Iman Taraghi[1,2], Anna Szymczyk[3], Elżbieta Piesowicz[1] and Zbigniew Rosłaniec[1]

*Address all correspondence to: spaszkiewicz@zut.edu.pl

1 Institute of Materials Science and Engineering, Faculty of Mechanical Engineering and Mechatronics, West Pomeranian University of Technology, Szczecin, Poland

2 Department of Mechanical Engineering, Semnan University, Semnan, Iran

3 Institute of Physics, Faculty of Mechanical Engineering and Mechatronics, West Pomeranian University of Technology, Szczecin , Poland

References

[1] Adams RK, Hoeschele GK, Witsiepe WK. Thermoplastic polyether-ester elastomers. In: Holden G, Kricheldorf HR, Quirck RP. Thermoplastic Elastomers. 2nd ed. Munich: Hanser; 2004. p. 183-216

[2] Gabriëlse W, Soliman M, Dijkstra K. Microstructure and phase behavior of block copoly(ether-ester) thermoplastic elastomers. Macromolecules. 2001;**34**:1681693. DOI: 10.1021/ma0012696

[3] Schmalz H, Abetz V, Lange R, Soliman M. New thermoplastic elastomers by incorporation of non-polar soft segments in PBT based copolyesters. Macromolecules. 2001;**34**:795-800. DOI: 10.1021/ma001226p

[4] Roslaniec Z. Polyester thermoplastic elastomers: Synthesis, properties, and some applications. In: Fakirov S, editor. Handbook of Condensation Elastomers. Weinheim: Wiley-VCH; 2005. p. 77-116

[5] Szymczyk A, Senderek E, Nastalczyk J, Roslaniec Z. New multiblock poly(ether-ester)s based on poly(trimethylene terephthalate) as rigid segments. European Polymer Journal. 2008;**44**:436-443. DOI: 10.1016/j.eurpolymj.2007.11.005

[6] Koerner H, Price G, Pearce NA, Alexander M, Vaia RA. Remotely actuated polymer nanocomposites-stress-recovery of carbon-nanotube-filled thermoplastic elastomers. Nature Materials. 2004;**3**:115-120. DOI: 10.1038/nmat1059

[7] Szymczyk A. Poly(trimethylene terephthalate-block-tetramethylene oxide) elastomer/single-walled carbon nanotubes nanocomposites: Synthesis, structure, and properties. Journal of Applied Polymer Science. 2012;**126**:796-807. DOI: 10.1002/app.36961

[8] Taraghi I, Fereidoon A, Paszkiewicz S, Roslaniec Z. Electrically conductive polycarbonate/ethylene-propylene copolymer/multi-walled carbon nanotubes nanocomposites with improved mechanical properties. Journal of Applied Polymer Science. 2017;**134**:44661. DOI: 10.1002/app.44661

[9] Guskos N, Maryniak M, Typek J, Guskos A, Szymczak R, Senderek E, Roslaniec Z, Petridis D, Aidinis K, Influence of maghemite concentration on magnetic interactions in maghemite/PTT-block-PTMO nanocomposite. Journal of Non-Crystalline Solids. 2008;**354**: 4401-4406. DOI: 10.1016/j.jnoncrysol.2008.06.059

[10] Paszkiewicz S, Szymczyk A, Pilawka R, Przybyszewski B, Czulak A, Rosłaniec Z. Improved thermal conductivity of poly(trimethylene terephthalate-block-poly(tetramethylene oxide) based nanocomposites containing hybrid single-walled carbon nanotubes/graphene nanoplatelets fillers. Advances in Polymer Technology. DOI: 10.1002/adv.21611

[11] Paszkiewicz S, Szymczyk A, Livanov K, Wagner HD, Rosłaniec Z. Enhanced thermal and mechanical properties of poly(trimethylene terephthalate-block-poly(tetramethylene oxide) segmented copolymer based hybrid nanocomposites prepared by in situ polymerization via synergy effect between SWCNTs and graphene nanoplatelets. eXPRESS Polymer Letters. 2015;**9**:509-524. DOI: 10.3144/expresspolymlett.2015.49

[12] Paszkiewicz S, Szymczyk A, Sui XM, Wagner HD, Linares A, Ezquerra TA, Rosłaniec Z, Synergetic effect of single-walled carbon nanotubes (SWCNT) and graphene nanoplatelets (GNP) in electrically conductive PTT-block-PTMO hybrid nanocomposites prepared by in situ polymerization. Composites Science and Technology. 2015;**118**:72-77. DOI: 10.1016/j.compscitech.2015.08.011

[13] Paszkiewicz S, Pawelec I, Szymczyk A, Rosłaniec Z. Thermoplastic elastomers containing 2D nanofillers: montmorillonite, graphene nanoplatelets and oxidized graphene platelets. Polish Journal of Chemical Technology. 2015;**17**:74-81. DOI: 10.1515/pjct-2015-0071

[14] Paszkiewicz S, Szymczyk A, Špitalsky Z, Mosnáček J, Kwiatkowski K, Rosłaniec Z. Structure and properties of nanocomposites based on PTT-block-PTMO copolymer and graphene oxide prepared by in situ polymerization. European Polymer Journal. 2014;**50**:69-77. DOI: 10.1016/j.eurpolymj.2013.10.031

[15] Paszkiewicz S, Pilawka R, Dudziec B, Dutkiewicz M, Marciniec B, Kochmańska A, Jedrzejewski R, Roslaniec Z. Morphology and phase separation in PTT-block-PTMO nanocomposites containing POSS particles. European Polymer Journal. 2015;**70**:37-44. DOI: 10.1016/j.eurpolymj.2015.07.004

[16] Szymczyk A, Paszkiewicz S, Rosłaniec Z. Influence of intercalated organoclay on the phase structure and physical properties of PTT-PTMO block copolymers. Polymer Bulletin. 2013;**70**:1575-1590. DOI: 10.1007/s00289-012-0859-y

[17] Kovacs JZ, Velegala BS, Schulte K, Bauhofer W. Two percolation thresholds in carbon nanotube epoxy composites. Composites Science and Technology. 2007;**67**:922-928. DOI: 10.1016/j.compscitech.2006.02.037

[18] Kim H, Abdala AA, Macosko CW. Graphene/polymer nanocomposites. Macromolecules. 2010;**43**:6515-6530. DOI: 10.1021/ma100572e

[19] Coleman JN, Khan U, Blau WJ, Gun'ko YK. Small but strong: a review of the mechanical properties of carbon nanotube polymer composites. Carbon. 2006;**44**:1624-1652. DOI: 10.1016/j.carbon.2006.02.038

[20] Moniruzzaman M, Winey KI. Polymer nanocomposites containing carbon nanotubes. Macromolecules. 2006;**39**:5194-5205. DOI: 10.1021/ma060733p

[21] Naderi G, Lafleur PG, Dubois C. Microstructure-properties correlations in dynamically vulcanized nanocomposite thermoplastic elastomers based on PP/EPDM. Polymer Engineering and Science. 2007;**47**:207-217. DOI: 10.1002/pen.20673

[22] www.dupont.com [Internet]. [Accessed: 1.02.2017]

[23] Guo Z, Kim TY, Lei K, Pereira T, Sugar JG, Hahn HT. Strengthening and thermal stabilization of polyurethane nanocomposites with silicon carbide nanoparticles by a surface initiated-polymerization approach. Composite Science and Technology. 2008;**68**:164-170. DOI: 10.1016/j.compscitech.2007.05.031

[24] Mavinakuli P, Wei S, Wang Q, Karki AB, Dhage S, Wang Z, Young DP, Guo Z. Polypyrrole/silicon carbide nanocomposites with tunable electrical conductivity. Journal of Physical Chemistry C. 2010;**114**:3874-3882. DOI: 10.1021/jp911766y

[25] Kueseng K, Jacob KI. Natural rubber nanocomposites with SiC nanoparticles and carbon nanotubes. European Polymer Journal. 2006;**42**:220-227. DOI: 10.1016/j.eurpolymj.2005.05.011

[26] Paszkiewicz S, Taraghi I, Szymczyk A, Huczko A, Kurcz M, Przybyszewski B, Stanik R, Linares A, Ezquerra TA, Rosłaniec Z, Electrically and thermally conductive thin elastic polymer foils containing SiC nanofibers. Composite Science and Technology. 2016. Forthcoming

[27] Špitalský Z, Danko M, Mosnáček J. Preparation of functionalized graphene sheets. Current Organic Chemistry. 2011;**15**:1133-1150. DOI: 10.2174/138527211795202988

[28] Loos J, Alexeev A, Grossiord N, Koning CE, Regev O. Visualization of single-wall carbon nanotube (SWNT) networks in conductive polystyrene nanocomposites by charge contrast imaging. Ultramicroscopy. 2005;**104**:160-167. DOI: 10.1016/j.ultramic.2005.03.007

[29] Kovacs JZ, Andersen K, Pauls JR, Garcia CP, Schossig M, Schulte K, Bauhofer W. Analyzing the quality of carbon nanotube dispersions in polymers using scanning electron microscopy. Carbon. 2007;**45**:1279-1288. DOI: 10.1016/j.carbon.2007.01.012

[30] Battistella M, Cascione M, Fiedler B, Wichmann MHG, Quaresimin M, SChulte K, Fracture behaviour of fumed silica/epoxy nanocomposites. Composites Part A —Applied Science and Manufacturing. 2008;**39**:1851-1858. DOI: 10.1016/j.compositesa.2008.09.010

[31] Khaderbad MA, Tjoa W, Oo TZ, Wei J, Sheri M, Mangalampalli R, Rao VR, Mhaisalkar SG, Mathews N. Facile fabrication of graphene devices through metalloporphyrin induced photocatalytic reduction. RSC Advances. 2012;**2**:4120-4124. DOI: 10.1039/C2RA00792D

[32] Bo Z, Shuai X, Mao S, Yang H, Qian J, Chen J, Yan J, Cen K. Green preparation of reduced graphene oxide for sensing and energy storage applications. Scientific Reports. 2014;**4**:4684. DOI: 10.1038/srep04684

[33] Stankovich S, Dikin DA, Piner RD, Kohlhaas KA, Kleinhammes A, Jia Y, Wu Y, Nguyen SBT, Ruoff RS. Synthesis of graphene-based nanosheets via chemical reduction of exfoliated graphite oxide. Carbon. 2007;**45**:1558-1565. DOI: 10.1016/j.carbon.2007.02.034

[34] Schniepp HC, Li JL, McAllister MJ, Sai H, Herrera-Alonso M, Adamson DH, Prud'homme RK, Car R, Saville DA, Aksay IA. Functionalized single graphene sheets derived from splitting graphite oxide. Journal of Physical Chemistry B. 2006;**110**:8535-8539. DOI: 10.1021/jp060936f

[35] Si YC, Samulski ET. Synthesis of water soluble graphene. Nano Letters. 2008;**8**:1679-1682. DOI: 10.1021/nl080604h

[36] Kwon J, Kim H. Comparison of the properties of waterborne polyurethane/multiwalled carbon nanotube and acid-treated multiwalled carbon nanotube composites prepared by in situ polymerization. Journal of Polymer Science: Part A: Polymer Chemistry. 2005;**43**:3973-3985. DOI: 10.1002/pola.20897

[37] Xiong J, Zheng Z, Qin X, Li M, Li H, Wang X. The thermal and mechanical properties of a polyurethane/multi-walled carbon nanotube composite. Carbon. 2006;**44**:2701-2707. DOI: 10.1016/j.carbon.2006.04.005

[38] Li J, Wang X, Yang C, Yang J, Wang Y, Zhang J. Toughening modification of polycarbonate/poly(butylene terephthalate) blends achieved by simultaneous addition of elastomer particles and carbon nanotubes. Composites Part A: Applied Science and Manufacturing. 2016;**90**:200-210. DOI: 10.1016/j.compositesa.2016.07.006

[39] Wang YH, Shi YY, Dai J, Yang JH, Huang T, Zhang N, Peng Y, Wang Y. Morphology and property changes of immiscible polycarbonate/poly(L-lactide) blends induced by carbon nanotubes. Polymer International. 2013;**62**:957-965. DOI: 10.1002/pi.4383

[40] Valentini L, Biagiotti J, Lopez-Manchado MA, Santucci S, Kenny JM. Effects of carbon nanotubes on the crystallization behavior of polypropylene. Polymer Engineering and Science. 2004;**44**:303-311. DOI: 10.1002/pen.20028

[41] Bhattacharyya AR, Sreekumar TV, Liu T, Kumar S, Ericson LM, Hauge RH, Smalley RE. Crystallization and orientation studies in polypropylene/single wall carbon nanotube composite. Polymer. 2003;**44**:2373-2377. DOI: 10.1016/S0032-3861(03)00073-9

[42] Anand KA, Agarwal US, Joseph R. Carbon nanotubes induced crystallization of poly(ethylene terephthalate). Polymer. 2006;**47**:3976-3980. DOI: 10.1016/j.polymer.2006.03.079

[43] Sun G, Chen G, Liu Z, Chen M. Preparation, crystallization, electrical conductivity and thermal stability of syndiotactic polystyrene/carbon nanotube composites. Carbon. 2010;**48**:1434-1440. DOI: 10.1016/j.carbon.2009.12.037

[44] Mitchell CM, Krishnamoorti R. Non-isothermal crystallization of in situ polymerized poly(ε-caprolactone) functionalized-SWNT nanocomposites. Polymer. 2005;**46**:8796-8804. DOI: 10.1016/j.polymer.2005.05.101

[45] Garcia-Gutierrez MC, Hernandez JJ, Nogales A, Panine P, Rueda DR, Ezquerra TA. Influence of shear on the templated crystallization of poly(butylene terephthalate)/single wall carbon nanotube nanocomposites. Macromolecules. 2008;**41**:844-851.DOI: 10.1021/ma0713512

[46] Cai Y, Chen L, Yang H, Gou J, Cheng L, Yin X, Yin H. Mechanical and electrical properties of carbon nanotube buckypaper reinforced silicon carbide nanocomposites. Ceramics International. 2016;**42**:4984-4992. DOI: 10.1016/j.ceramint.2015.12.011

[47] Dresselhaus MS, Dresselhaus G, Saito R. Physics of carbon nanotubes. Carbon. 1995;**33**:883-891. DOI: 10.1016/0008-6223(95)00017-8

[48] Chae HG, Liu J, Kumar S. Carbon nanotubes-enabled materials. In: O'Connell MJ, editor. Carbon Nanotubes Properties and Applications. Boca Raton: CRC Press Taylor and Francis Group; 2006. p. 213-253

[49] Cooper CA, Young RJ, Halsall M. Investigation into the deformation of carbon nanotubes and their composites through the use of Raman spectroscopy. Composites Part A: Applied Science and Manufacturing. 2001;**32A**:401-411. DOI: 10.1016/S1359-835X(00)00107-X

[50] Dumitrica T, Hua M, Yakobson BI. Symmetry-, time-, and -dependent strength of carbon nanotubes. Proceedings of National Academy of Sciences of the United States of America. 2006;**103**:6105-6109. DOI: 10.1073/pnas.0600945103

[51] Monthioux M. Filling single-wall carbon nanotubes. Carbon. 2002;**40**:1809-1823. DOI: 10.1016/S0008-6223(02)00102-1

[52] Slonczewski JC, Weiss PR. Band structure of graphite. Physical Review. 1958;**109**:272. DOI: 10.1103/PhysRev.109.272

[53] Novoselov KS, Geim AK, Morozov SV, Jiang D, Zhang Y, Dubonos SV, Grigorieva IV, Firsov AA. Electric field effect in atomically thin carbon films. Science. 2004;**306**:666-669. DOI: 10.1126/science.1102896

[54] Lee C, Wei X, Kysar JW, Hone J. Measurement of the elastic properties and intrinsic strength of monolayer graphene. Science. 2008;**321**:385-388. DOI: 10.1126/science.1157996

[55] Balandin AA, Ghosh S, Bao W, Calizo I, Teweldebrhan D, Miao F, Lau CN. Superior thermal conductivity of single-layer graphene. Nano Letters. 2008;**8**:902-907. DOI: 10.1021/nl0731872

[56] Hernández JJ, García-Gutiérrez MC, Nogales A, Rueda DR, Kwiatkowska M, Szymczyk A, Roslaniec Z, Concheso A, Guinea I, Ezquerra TA. Influence of preparation procedure on the conductivity and transparency of SWCNT-polymer nanocomposites. Composites Science and Technology. 2009;**69**:1867-1872. DOI: 10.1016/j.compscitech.2009.04.002

[57] Szymczyk A, Roslaniec Z, Zenker M, Garcia-Gutierez MC, Hernandez JJ, Rueda DR, Nogales A, Ezquerra TA. Preparation and characterization of nanocomposites based on COOH functionalized multi-walled carbon nanotubes and on poly(trimetylene terephthalate. eXPRESS Polymer Letters. 2011;**5**:977-995. DOI: 10.3144/expresspolymlett.2011.96

[58] Paszkiewicz S, Szymczyk A, Špitalský Z, Soccio M, Mosnáček J, Ezquerra TA, Rosłaniec Z. Electrical conductivity of PET/expanded graphite nanocomposites prepared by in situ polymerization. Journal of Polymer Science. Part B: Polymer Physics. 2012;**50**:1645-1652. DOI: 10.1002/polb.23176

[59] Paszkiewicz S. Multifunctional polymer nanocomposites based on thermoplastic polyester. In: Farrukh MA, editor. Functionalized Nanomaterials. Croatia: InTech; 2016. DOI: 10.5772/63186

[60] Watanabe M. Nagaoka K, Kanba M, Shinohara I. Ionic conductivity of polymeric solid electrolytes based on (polypropoylene oxide) and poly(tetramathylene oxide). Polymer Journal. 1982;**14**:877-886.DOI: 10.1295/polymj.14.877

[61] Kuo SW, Chang FC. POSS related polymer nanocomposites. Progress in Polymer Science. 2011;**36**:1649-1696. DOI: 10.1016/j.progpolymsci.2011.05.002

[62] Ayandele E, Sarkar B, Alexandridis P. Polyhedral oligomeric silsesquioxane (POSS)-containing polymer nanocomposites. Nanomaterials. 2012;**2**:445-475. DOI: 10.3390/nano2040445

[63] Nezakati T, Tan A, Seifalian AA. Enhancing the electrical conductivity of a hybrid POSS-PCL/graphene nanocomposite polymer. Journal of Colloid Interface Science. 2014;**435**:145-155. DOI: 10.1016/j.jcis.2014.08.020

[64] Zhang SM, Lin L, Deng H, Gao X, Bilotti E, Peijs T, Zhang Q, Fu Q. Synergistic effect in conductive networks constructed with carbon nanofillers in different dimensions. eXPRESS Polymer Letters. 2012;**6**:159-168. DOI: 10.3144/expresspolymlett.2012.17

[65] Sandler J, Shaffer MSP, Prasse T, Bauhofer W, Schulte K, Windle AH. Development of a dispersion process for carbon nanotubes in an epoxy matrix and the resulting electrical properties. Polymer. 1999;**40**:5967-5971.DOI: 10.1016/S0032-3861(99)00166-4

[66] Fu F, Scogna RC, Zhou W, Brand S, Fischer JE, Winey KI. Nanotube networks in polymer nanocomposites: rheology and electrical conductivity. Macromolecules. 2004;**37**:9048-9055. DOI: 10.1021/ma049164g

[67] Stauffer D. Scaling theory of percolation clusters. Physics Reports. 1979;**54**:1-74. DOI: 10.1016/0370-1573(79)90060-7

[68] Stauffer D, Aharony A. Introduction to percolation theory. 1st ed. London: Taylor and Francis; 1992

[69] Paszkiewicz S. Polymer hybrid nanocomposites containing carbon nanoparticles. In situ synthesis and physical properties [PhD dissertation]. Szczecin: West Pomeranian University of Technology; 2014. 190 p

[70] www.sigma-aldrich.com [Internet]. [Accessed: 2017-02-5]

[71] www.nanocs.com [Internet]. [Accessed: 2017-02-7]

[72] Zeynalov EB., Friedrich JF. Antioxidative activity of carbon nanotube and nanofiber. The Open Materials Science Journal. 2008;**2**:28-34. DOI: 10.2174/1874088X00802010028

[73] Szymczyk A, Rosłaniec Z. Degradacja i stabilizacja termoplastycznych elastomerów. Polimery. 2006;**51**:627-642

[74] Fakirov S, Roslaniec Z. Handbook of Condensation Thermoplastic Elastomers. Chapter 3 Polyester Thermoplastic Elastomers: Synthesis, Properties, and Some Applications. Weinheim: Wiley-VCH Verlag GmbH & Co. KGaA; 2005